

Y. Okamoto, MD  
M. Ihara, MD, PhD,  
FACP  
M. Urushitani, MD, PhD  
H. Yamashita, MD, PhD  
T. Kondo, MD  
A. Tanigaki  
M. Oono, MD  
J. Kawamata, MD, PhD  
A. Ikemoto, MD, PhD  
Y. Kawamoto, MD, PhD  
R. Takahashi, MD, PhD  
H. Ito, MD, PhD

## AN AUTOPSY CASE OF *SOD1*-RELATED ALS WITH TDP-43 POSITIVE INCLUSIONS

Approximately 20% of familial amyotrophic lateral sclerosis (FALS) cases are linked to mutations in the antioxidant enzyme, *Cu/Zn superoxide dismutase (SOD1)*. Controversy exists as to whether *SOD1*-related FALS and sporadic ALS (SALS) share common mechanistic pathways, since very few *SOD1*-related FALS cases exhibit cytoplasmic inclusions composed of 43-kDa TAR DNA-binding protein (TDP-43), a pathologic hallmark of SALS and *SOD1*-unrelated FALS.<sup>1,2,e1,e2</sup> We describe prominent TDP-43 pathology in the spinal cord of a patient with *SOD1*-related ALS with *SOD1* I112T mutation, a relatively uncommon variant form leading to rapid disease progression.<sup>3</sup>

**Case report.** A 41-year-old man with no familial history of neurodegenerative disorder noted progressive weakness in his left leg. Four months after onset, a neurologic examination detected muscle weakness in the left lower extremity and fasciculation in all the extremities. Tendon reflexes were decreased and Babinski sign was negative bilaterally; EMG revealed a neurogenic pattern in the left extremities. Dysarthria and dysphagia were not evident. He was diagnosed with ALS. Within a year, he became bedridden and died at the age of 43 because of respiratory failure. Genomic DNA was extracted from the autopsied samples with informed consent from his family. DNA analysis revealed a missense mutation (I112T) in *SOD1* gene (figure 1A). Mutations were not found in other exons of *SOD1* gene or in the *TDP-43* gene. The prefixed brain weighed 1,400 g with no apparent abnormalities in external appearance. Microscopic examination revealed marked loss of motor neurons, with glial proliferation in the spinal cord and Lewy body–like hyaline inclusions found in the remaining motor neurons; Bunina bodies were not observed. Myelin pallor was evident in the corticospinal tract, the middle root zone of the posterior column, and the spinocerebellar tract (figure e-1 on the *Neurology*<sup>®</sup> Web site at [www.neurology.org](http://www.neurology.org)). Immunohistochemical analysis was performed with antibodies specific to anti-misfolded *SOD1* (D3H5),<sup>4,5</sup> anti-*SOD1* (SOD-100), anti-phosphorylated TDP-43

(pTDP-43), and anti-nonphosphorylated TDP-43 (TDP-43) (table e-1). Inclusions immunopositive for D3H5 or pTDP-43 were undetectable in the brain, except for the brainstem or spinal cord. D3H5 immunoreactivity was more intense and more diffusely distributed than that of SOD-100. Numerous D3H5-positive inclusions were observed in brainstem nuclei, including the hypoglossal nucleus and reticular formation of the medulla oblongata (figure 1, B and C). D3H5-positive inclusions were less frequently present in the anterior horn cells of the cervical spinal cord (figure 1D); however, they were not found in the lumbar spinal cord (figure 1E). In contrast, pathologic pTDP-43 immunoreactivity was not found in the brainstem (figure 1, F and G) or cervical spinal cord (figure 1H), whereas abundant pTDP-43-positive inclusions were present in the neuronal cytoplasm (figure 1I) or glial cells (figure 1, J and K) of the lumbar spinal cord. The topographic distributions of D3H5 and pTDP-43 immunoreactivity were apparently distinct, and double immunofluorescent staining revealed that D3H5 did not colocalize with pTDP-43 (figure 1, L–N) or TDP-43 (figure 1, O–Q).

D3H5-immunoreactive inclusions were not detectable in the lumbar anterior horn cells of a SALS case or 2 non-ALS disease control cases (figure e-2).

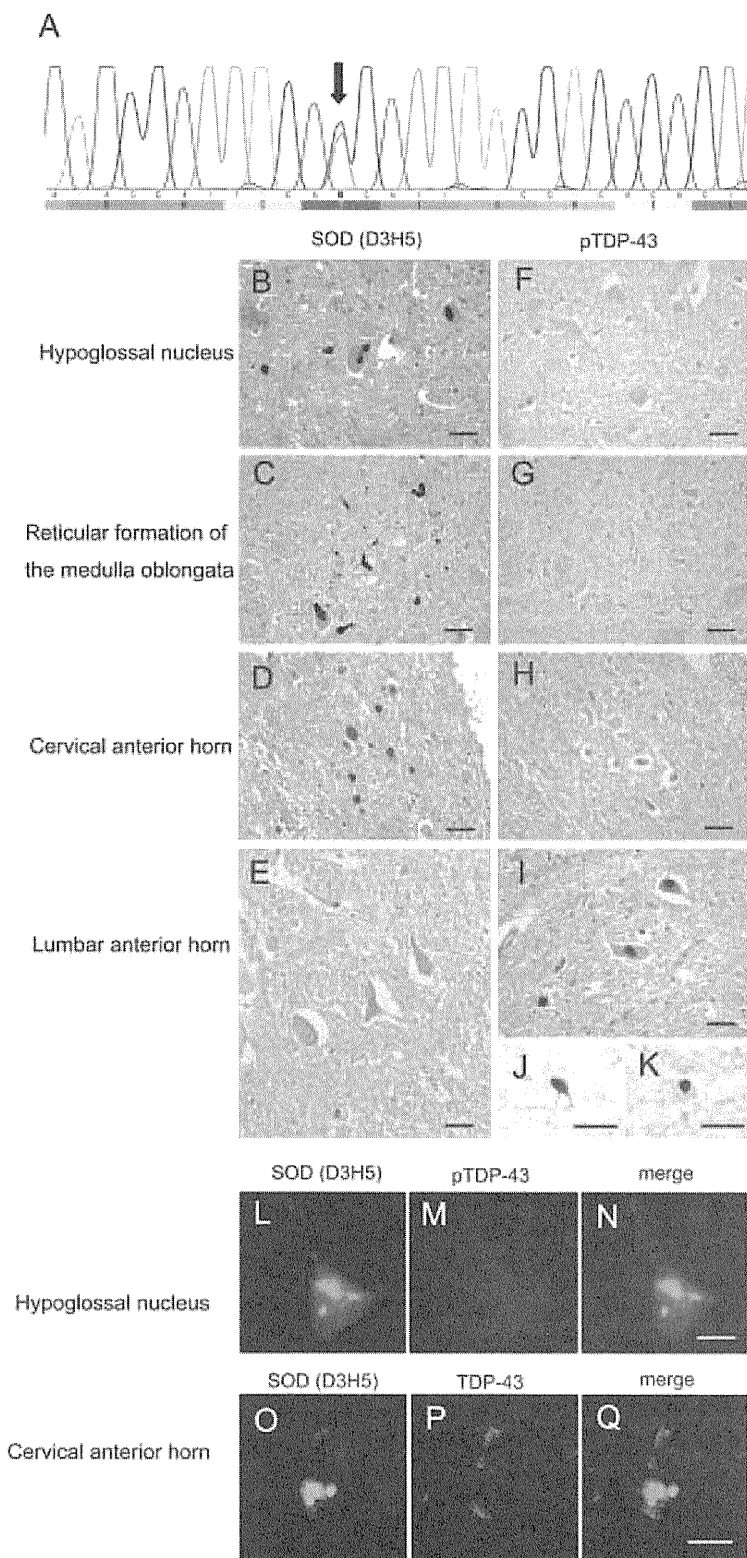
**Discussion.** The relative paucity of cytoplasmic TDP-43 inclusions in mutant *SOD1*-related FALS cases<sup>2,e2</sup> suggests that the 2 pathogenic pathways are unrelated. Nevertheless, the present ALS case with a mutation in *SOD1* exhibits typical TDP-43 pathology, including the presence of neuronal and glial cytoplasmic inclusions. Two previously reported *SOD1*-related FALS cases (C111Y and H48Q) have reported a few TDP-43 inclusions in the neuronal cytoplasm.<sup>6,e3</sup> In one case, TDP-43 colocalized with *SOD1*, suggesting that TDP-43 is sequestered into *SOD1* aggregation<sup>6</sup>; while in the other study, the TDP-43 immunoreactivity was only present in a single neuron, with no reference to colocalization of TDP-43 with *SOD1*.<sup>e3</sup> The striking feature in our patient is that misfolded *SOD1* and pTDP-43 aggregates were both present, though mutually exclusive.

Supplemental data at  
[www.neurology.org](http://www.neurology.org)

Supplemental Data



**Figure 1 Genetic and neuropathologic data**



Heterozygous point mutation (1,144 T>C) in exon 4, resulting in amino acid substitution of isoleucine to threonine at the 112th residue (A, arrow). Mutually exclusive patterns of D3H5 and pTDP-43 immunoreactivity in the brainstem and spinal cord areas indicated (B–K). Noncolocalization of D3H5 with pTDP-43 (L–N) or TDP-43 (O–Q) in the hypoglossal nucleus and cervical cord. Autofluorescence associated with lipofuscin granules (P, Q). Bars, 40  $\mu\text{m}$  (B–H, L–Q) and 20  $\mu\text{m}$  (I–K).

Given that misfolded SOD1 oxidized at C111 residue is found even in SALS,<sup>7</sup> it appears that pathogenesis of SOD1-related FALS and SALS might converge on a common pathway. Further genotype–phenotype correlation needs to be investigated to elucidate the linkage, if any, between the SOD1 and TDP-43 mechanistic pathways involved in ALS.

From the Department of Neurology (Y.O., M.I., H.Y., T.K., A.T., M.O., A.I., Y.K., R.T., H.I.), Kyoto University Graduate School of Medicine, Kyoto; Molecular Neuroscience Research Center (M.U., M.O.), Shiga University of Medical Science, Shiga; and Department of Neurology (J.K.), Sapporo Medical University, Sapporo, Japan.

References e1–e3 are available on the Neurology® Web site at [www.neurology.org](http://www.neurology.org).

Author contributions: Dr. Okamoto: data collection, pathological analysis, and manuscript writing. Dr. Ihara: planning, analysis, interpretation, manuscript writing and editing, and administrative support. Dr. Urushitani: establishment and purification of antibody and supervision. Dr. Yamashita: advice on double immunofluorescence. Dr. Kondo: genetic analysis and data interpretation. A. Tanigaki: genetic analysis. Dr. Oono: purification of antibody. Dr. Kawamata: genetic analysis and patient care. Dr. Ikemoto: patient care. Dr. Kawamoto: pathological diagnosis. Dr. Takahashi: data interpretation. Dr. Ito: data interpretation.

Disclosure: Dr. Okamoto, Dr. Ihara, Dr. Urushitani, Dr. Yamashita, Dr. Kondo, A. Tanigaki, Dr. Oono, Dr. Kawamata, Dr. Ikemoto, and Dr. Kawamoto report no disclosures. Dr. Takahashi serves on scientific advisory boards for FP Pharmaceuticals, LLC, Daiichi Sankyo, and the Ministry of Education, Culture, Sports, Science and Technology, Japan; has received speaker honoraria for Novartis, Boehringer Ingelheim, GlaxoSmithKline, Dainippon Sumitomo Pharma, and FP Pharmaceuticals, LLC; serves on the editorial boards of Neuroscience Research and the Journal of Neural Transmission; holds patents re: The use of mutant mouse of Chimerin for drug screening and Drug screening using iPS cells; and receives research support from Novartis, Boehringer Ingelheim, GlaxoSmithKline, Dainippon Sumitomo Pharma, FP Pharmaceuticals, LLC, the Ministry of Education, Culture, Sports, Science and Technology, Japan, the Ministry of Health, Labor and Welfare, Japan, and the Japan Science and Technology Agency. Dr. Ito reports no disclosures.

Address correspondence and reprint requests to Dr. Masafumi Ihara, Department of Neurology, Kyoto University Graduate School of Medicine, 54 Kawabaracho Shogoin Sakyo-ku, Kyoto City, Kyoto, 6068507, Japan; [ihara@kuhp.kyoto-u.ac.jp](mailto:ihara@kuhp.kyoto-u.ac.jp)

Received March 28, 2011. Accepted in final form August 12, 2011.

Copyright © 2011 by AAN Enterprises, Inc.

1. Neumann M, Sampathu DM, Kwong LK, et al. Ubiquitinated TDP-43 in frontotemporal lobar degeneration and amyotrophic lateral sclerosis. *Science* 2006;314:130–133.
2. Tan CF, Eguchi H, Tagawa A, et al. TDP-43 immunoreactivity in neuronal inclusions in familial amyotrophic lateral sclerosis with or without SOD1 gene mutation. *Acta Neuropathol* 2007;113:535–542.
3. Cudkowicz ME, McKenna-Yasek D, Sapp PE, et al. Epidemiology of mutations in superoxide dismutase in amyotrophic lateral sclerosis. *Ann Neurol* 1997;41:210–221.
4. Urushitani M, Ezzi SA, Julien JP. Therapeutic effects of immunization with mutant superoxide dismutase in mice models of amyotrophic lateral sclerosis. *Proc Natl Acad Sci USA* 2007;104:2495–2500.

5. Gros-Louis F, Soucy G, Lariviere R, Julien JP. Intracerebroventricular infusion of monoclonal antibody or its derived Fab fragment against misfolded forms of SOD1 mutant delays mortality in a mouse model of ALS. *J Neurochem* 2010;113:1188–1199.
6. Sumi H, Kato S, Mochimaru Y, Fujimura H, Etoh M, Sakoda S. Nuclear TAR DNA binding protein 43 expression in spinal cord neurons correlates with the clinical course in amyotrophic lateral sclerosis. *J Neuropathol Exp Neurol* 2009;68:37–47.
7. Bosco DA, Morfini G, Karabacak NM, et al. Wild-type and mutant SOD1 share an aberrant conformation and a common pathogenic pathway in ALS. *Nat Neurosci* 2010;13:1396–1403.

## Ramp Up Your Self-assessment with NeuroSAE<sup>®</sup>

We've ramped up the benefits without ramping up the price. That's right. In addition to meeting the self-assessment requirements for MOC, NeuroSAE IV now offers 6 CME credits to help fulfill both the self-assessment and CME requirements of your ABPN-required maintenance of certification.

- Assess your knowledge of neurology
- Compare your performance to other neurologists
- Use convenient online program
- Access from your mobile phone

Get started today at [www.aan.com/view/NeuroSAE](http://www.aan.com/view/NeuroSAE)

## Call for Nominations: Editor-in-Chief, *Continuum: Lifelong Learning in Neurology*

The Editorial Search Committee for *Continuum: Lifelong Learning in Neurology*<sup>®</sup> is requesting that AAN members submit the names of eligible candidates for Editor-in-Chief of the Academy's premier self-study continuing medical education program. Self-nominations or nominations of other AAN members are encouraged. A position description, including requirements, is available at [www.aan.com/view/continuumeditor](http://www.aan.com/view/continuumeditor).

The Editor-in-Chief is responsible for publishing six issues of *Continuum*<sup>®</sup> a year. The appointment is six years beginning January 1, 2013, with a six-month transition with the current editor beginning July 2012. The Editorial Search Committee members are Robert C. Griggs, MD, FAAN, chair; Terrence L. Cascino, MD, FAAN; Bruce Sigsbee, MD, FAAN; Cynthia L. Comella, MD, FAAN; Robert A. Gross, MD, PhD, FAAN; and Steven P. Ringel, MD, FAAN.

Please submit current curriculum vitae with a letter outlining scientific editing experience, a vision for *Continuum's* role within the AAN, and an editorial vision for *Continuum* by November 30, 2011. All candidates will also be required to complete an AAN conflicts of interest disclosure. For more information, contact Andrea Weiss at [aweiss@aan.com](mailto:aweiss@aan.com) or (651) 695-2742.

Submit nominations to: Missy Render  
Administrator  
AAN Enterprises, Inc.  
1080 Montreal Avenue  
St. Paul, MN, 55116  
[mrender@aan.com](mailto:mrender@aan.com)

# Colocalization of 14-3-3 Proteins with SOD1 in Lewy Body-Like Hyaline Inclusions in Familial Amyotrophic Lateral Sclerosis Cases and the Animal Model

Yoko Okamoto<sup>1,9</sup>, Yoshitomo Shirakashi<sup>1,9</sup>, Masafumi Ihara<sup>1\*</sup>, Makoto Urushitani<sup>2</sup>, Miki Oono<sup>1,2</sup>, Yasuhiro Kawamoto<sup>1</sup>, Hirofumi Yamashita<sup>1</sup>, Shun Shimohama<sup>3</sup>, Shinsuke Kato<sup>4</sup>, Asao Hirano<sup>5</sup>, Hidekazu Tomimoto<sup>6</sup>, Hidefumi Ito<sup>1</sup>, Ryosuke Takahashi<sup>1</sup>

**1** Department of Neurology, Kyoto University Graduate School of Medicine, Kyoto, Japan, **2** Molecular Neuroscience Research Center, Shiga University of Medical Science, Shiga, Japan, **3** Department of Neurology, Sapporo Medical University School of Medicine, Hokkaido, Japan, **4** Department of Neuropathology, Institute of Neurological Sciences, Faculty of Medicine, Tottori University, Tottori, Japan, **5** Division of Neuropathology, Department of Pathology, Montefiore Medical Center, New York, New York, United States of America, **6** Department of Neurology, Mie University Graduate School of Medicine, Mie, Japan

## Abstract

**Background and Purpose:** Cu/Zn superoxide dismutase (SOD1) is a major component of Lewy body-like hyaline inclusion (LBHI) found in the postmortem tissue of SOD1-linked familial amyotrophic lateral sclerosis (FALS) patients. In our recent studies, 14-3-3 proteins have been found in the ubiquitinated inclusions inside the anterior horn cells of spinal cords with sporadic amyotrophic lateral sclerosis (ALS). To further investigate the role of 14-3-3 proteins in ALS, we performed immunohistochemical analysis of 14-3-3 proteins and compared their distributions with those of SOD1 in FALS patients and SOD1-overexpressing mice.

**Methods:** We examined the postmortem brains and the spinal cords of three FALS cases (A4V SOD1 mutant). Transgenic mice expressing the G93A mutant human SOD1 (mutant SOD1-Tg mice), transgenic mice expressing the wild-type human SOD1 (wild-type SOD1-Tg mice), and non-Tg wild-type mice were also subjected to the immunohistochemical analysis.

**Results:** In all the FALS patients, LBHIs were observed in the cytoplasm of the anterior horn cells, and these inclusions were immunopositive intensely for pan 14-3-3, 14-3-3 $\beta$ , and 14-3-3 $\gamma$ . In the mutant SOD1-Tg mice, a high degree of immunoreactivity for misfolded SOD1 (C4F6) was observed in the cytoplasm, with an even greater degree of immunoreactivity present in the cytoplasmic aggregates of the anterior horn cells in the lumbar spinal cord. Furthermore, we have found increased 14-3-3 $\beta$  and 14-3-3 $\gamma$  immunoreactivities in the mutant SOD1-Tg mice. Double immunofluorescent staining showed that C4F6 and 14-3-3 proteins were partially co-localized in the spinal cord with FALS and the mutant SOD1-Tg mice. In comparison, the wild-type SOD1-Tg and non-Tg wild-type mice showed no or faint immunoreactivity for C4F6 and 14-3-3 proteins (pan 14-3-3, 14-3-3 $\beta$ , and 14-3-3 $\gamma$ ) in any neuronal compartments.

**Discussion:** These results suggest that 14-3-3 proteins may be associated with the formation of SOD1-containing inclusions, in FALS patients and the mutant SOD1-Tg mice.

**Citation:** Okamoto Y, Shirakashi Y, Ihara M, Urushitani M, Oono M, et al. (2011) Colocalization of 14-3-3 Proteins with SOD1 in Lewy Body-Like Hyaline Inclusions in Familial Amyotrophic Lateral Sclerosis Cases and the Animal Model. PLoS ONE 6(5): e20427. doi:10.1371/journal.pone.0020427

**Editor:** Mel B. Feany, Brigham and Women's Hospital, Harvard Medical School, United States of America

**Received:** February 11, 2011; **Accepted:** April 27, 2011; **Published:** May 31, 2011

**Copyright:** © 2011 Okamoto et al. This is an open-access article distributed under the terms of the Creative Commons Attribution License, which permits unrestricted use, distribution, and reproduction in any medium, provided the original author and source are credited.

**Funding:** The authors have no support or funding to report.

**Competing Interests:** The authors have declared that no competing interests exist.

\* E-mail: ihara@kuhp.kyoto-u.ac.jp

<sup>9</sup> These authors contributed equally to this work.

## Introduction

Amyotrophic lateral sclerosis (ALS) is a fatal, progressive neurodegenerative disease characterized by the degeneration of motor neurons in the motor cortex, brainstem and spinal cord. The vast majority of ALS patients are sporadic, and approximately 5–10% of ALS cases are familial ALS (FALS) [1]. Among the FALS patients, approximately 20% are linked to mutations in the antioxidant enzyme Cu/Zn superoxide dismutase (SOD1) [2]. Mutant SOD1 proteins aggregate and form Lewy body-like

hyaline inclusions (LBHIs) in the anterior horn cells of the spinal cord [3].

Transgenic mice carrying several copies of human mutant SOD1 genes show ALS-like symptoms such as progressive motor disturbances and neurogenic amyotrophy, and develop a pathology resembling ALS [4]. In brief, these Tg mice demonstrate atrophy of the motor neuronal system, vacuolar degeneration of the motor neurons, and ubiquitinated neuronal hyaline inclusions which contain SOD1 in their cell bodies and swollen processes [5].

SOD1 is a major constituent of LBHIs linked to FALS, and these LBHIs contain ubiquitin [6], phosphorylated neurofilaments [7], and a copper chaperone for superoxide dismutase [8].

The 14-3-3 proteins, a family of protein chaperones, are abundant in the brain, comprising approximately 1% of the total brain protein [9]. 14-3-3 proteins consist of seven different isoforms, named with Greek letters ( $\beta$ ,  $\epsilon$ ,  $\gamma$ ,  $\eta$ ,  $\theta$ ,  $\sigma$ , and  $\zeta$ ). Each isoform forms homo- or hetero-dimers. 14-3-3 dimers can simultaneously bind two ligands, modulate different signaling molecules and participate in cell cycle control, cell adhesion, neuronal plasticity as well as various intracellular signal transduction pathways [10]. 14-3-3 proteins seem to control the subcellular localization of proteins and to function as adaptor molecules, stimulating protein-protein interactions. The regulation of this interaction usually involves the phosphorylation of the interacting proteins [11].

In our recent studies, several types of 14-3-3 proteins such as 14-3-3 $\beta$ , 14-3-3 $\gamma$ , 14-3-3 $\zeta$ , 14-3-3 $\theta$ , or 14-3-3 $\epsilon$  have been found in the ubiquitinated inclusions of anterior horn cells from patients with sporadic ALS [12]. 14-3-3 mRNA was also demonstrated to be upregulated in the spinal cords with sporadic ALS [13].

However, the association of 14-3-3 proteins with FALS remains unknown. In this study, to investigate the role of 14-3-3 proteins and SOD1 in the pathogenesis of FALS, we performed immunohistochemical staining for 14-3-3 proteins and SOD1 in formalin-fixed, paraffin-embedded sections from patients with FALS. Transgenic mice which overexpress mutant human SOD1, transgenic mice which overexpress wild type human SOD1, and non-transgenic wild-type mice were also subjected to immunohistochemical analysis.

## Methods

### Ethics Statement

The protocols for genetic analysis and neuropathological procedures were approved by and performed under the guidelines of our institutional ethics committee. Informed consent was obtained from all individuals or their guardians before the analysis. The animal study was carried out in strict accordance with the guidelines for animal experimentation from the Animal Research Committee of our institution. The protocol was approved by the Animal Research Committee, Kyoto University (Permit Number: MedKyo10202).

### Human FALS cases

We analyzed three cases of FALS (A4V SOD1 mutant). The clinicopathological backgrounds of these FALS cases have been previously reported [14]. These patients were members of the American "C" family. The three patients were males, and their ages at death were 39, 46 and 66 years. They were pathologically consistent with FALS with posterior column involvement [15].

### Transgenic mice expressing G93A mutant human SOD1 and wild type human SOD1

We used transgenic mice expressing the G93A mutant human SOD1 gene (mutant SOD1-Tg mice) [B6SJL-TgN (SOD1-G93A) 1Gur] and wild-type human SOD1 gene (wild-type SOD1-Tg mice) [B6SJL-Tg (SOD1) 2Gur/J], which were originally obtained from the Jackson Laboratory [16]. The mutant SOD1-Tg mice develop signs of hind limb weakness at the age of 3 to 4 months. At the age of 5 to 6 months, they are not able to forage for food and water and then die. The wild-type SOD1-Tg mice show no motor symptoms [17]. We analyzed four-month-old mutant SOD1-Tg and wild-type SOD1-Tg mice ( $n = 4$ , each).

### Human tissues

Human tissue blocks obtained from the different levels of spinal cords of FALS cases were embedded in paraffin. The blocks were sectioned with a microtome at 6  $\mu$ m thickness for routine and immunohistochemical staining. Routine histological assessment was carried out with hematoxylin and eosin (H&E).

H&E-stained sections with LBHIs were photographed, decolorized with 70% ethanol and pretreated with 0.3%  $H_2O_2$  in 0.1 mol/L phosphate-buffered saline (PBS) for 30 min at room temperature to inhibit any endogenous peroxidase activity. After washing with 0.1 mol/L PBS, these sections were blocked with 0.1 mol/L PBS plus 3% skim milk for 2 hours at room temperature. Then, the specimens were used for immunohistochemistry; this involved sequential incubation with primary antibody, appropriate biotinylated secondary antibody (Vector Laboratories, diluted 1:200), and avidin-biotin-peroxidase complex (ABC; Vector Laboratories, 1:200) in 0.1 mol/L PBS containing 0.3% Triton X-100 (PBST, pH 7.4). The sections were rinsed with PBST for 15 min between each step and finally visualized with 0.01% diaminobenzidine tetrahydrochloride and 0.005%  $H_2O_2$  in 50 mmol/L Tris-HCl (pH 7.6).

### Animal tissues

Mice were deeply anesthetized with sodium pentobarbital and were perfused transcardially with 0.01 mol/L PBS and then with a fixative containing 4% paraformaldehyde (PFA) and 0.2% picric acid in 0.1 mol/L phosphate buffer (PB, pH 7.4). Then, the brains and the spinal cords were removed. The tissues were post-fixed for 24 hours in 4% PFA and stored in 20% sucrose in 0.1 mol/L PB (pH 7.4). Serial lumbar spinal sections were cut into 20  $\mu$ m thick sections on a cryostat, and immunohistochemical analysis was performed in the same way as human tissues described above.

**Table 1. Primary antibodies.**

Primary antibody	Company	Dilution
C4F6 mouse monoclonal	Reference [18]	1:1000
SOD1 goat polyclonal C-17 SC-8637	Santa Cruz Biotechnology	1:1000
pan 14-3-3 mouse monoclonal H-8 SC-1657	Santa Cruz Biotechnology	1:1000
14-3-3 $\beta$ rabbit polyclonal C-20 SC-628	Santa Cruz Biotechnology	1:2000
14-3-3 $\gamma$ rabbit polyclonal C-16 SC-731	Santa Cruz Biotechnology	1:2000
14-3-3 $\epsilon$ rabbit polyclonal T-16 SC-1020	Santa Cruz Biotechnology	1:400
14-3-3 $\eta$ goat polyclonal E-12 SC-17287	Santa Cruz Biotechnology	1:400
14-3-3 $\theta$ rabbit polyclonal C-17 SC-732	Santa Cruz Biotechnology	1:2000
14-3-3 $\sigma$ goat polyclonal C-18 SC-7683	Santa Cruz Biotechnology	1:400
14-3-3 $\sigma$ goat polyclonal N-14 SC-7681	Santa Cruz Biotechnology	1:400
14-3-3 $\zeta$ rabbit polyclonal C-16 SC-1019	Santa Cruz Biotechnology	1:2000

doi:10.1371/journal.pone.0020427.t001

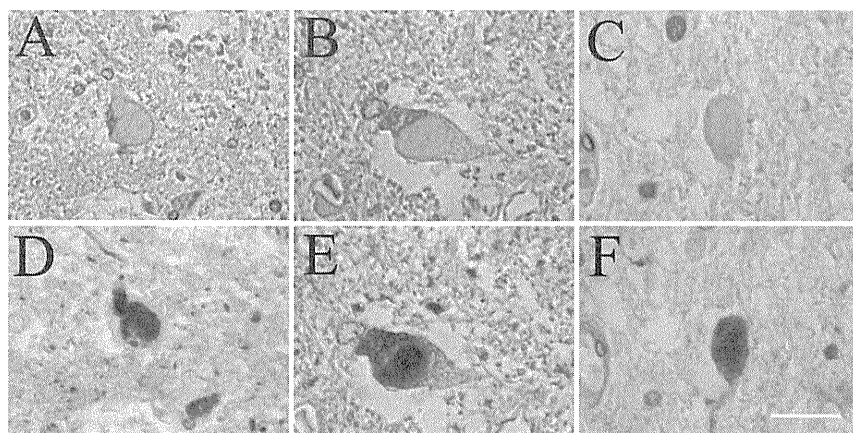


**Figure 1. LBHIs immunopositive for 14-3-3 proteins in FALS patients.** A, B, and C are the same sections as D, E, and F, respectively. The upper panels (A–C) are stained with H&E, and the lower panels (D–F) are immunostained with the anti-pan 14-3-3 antibody. LBHIs observed on H&E in the anterior horn cells are intensely immunopositive for pan 14-3-3. Bar indicates 100  $\mu$ m in (A, D), and 50  $\mu$ m in (B, C, E, F).  
doi:10.1371/journal.pone.0020427.g001

#### Primary antibodies

As primary antibodies, we used anti-SOD1, anti-misfolded SOD1 (C4F6) [18], and anti-pan and isoform-specific 14-3-3 protein antibodies. The primary antibodies used were listed in Table 1.

#### Double labeling immunohistochemistry

To investigate the relationship between SOD1 and 14-3-3 proteins, spinal cord sections of the FALS cases were incubated with primary antibodies against SOD1 and pan 14-3-3, followed by incubation with FITC- or rhodamine-labeled appropriate secondary antibodies. For mouse tissues, anti-14-3-3 ( $\beta$  or  $\gamma$ ) and C4F6-DyLight 488 antibodies were used. C4F6 was labeled with

DyLight Fluor 488 using a commercially available kit (DyLight Microscale Antibody Labeling Kits, Thermo Scientific).

#### Results

##### 14-3-3 immunoreactivity in patients with FALS

In all the three FALS cases, LBHIs were observed inside the anterior horn cells (Figure 1A–C). All the LBHIs observed on H&E showed strong pan 14-3-3 immunoreactivity (Figure 1D–F). Using 14-3-3 isoform-specific antibodies, all the LBHIs detected by H&E (Figure 2A, B) were intensely immunopositive both for 14-3-3 $\beta$  (Figure 2C) and 14-3-3 $\gamma$  (Figure 2D).

Double immunofluorescent-stained sections showed that pan 14-3-3 was co-localized with SOD1 in the LBHI (Figure 3).

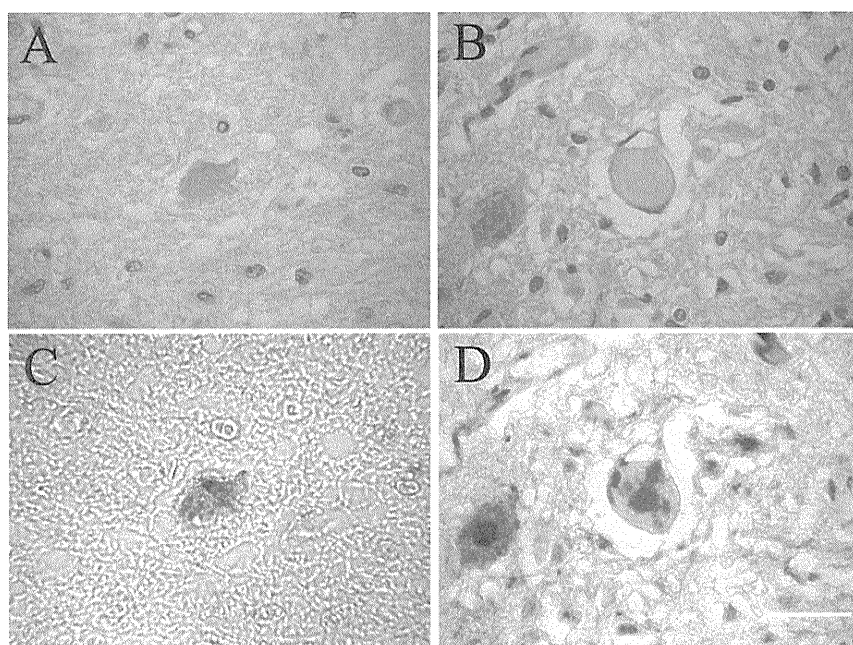


**Figure 2. LBHIs immunopositive for 14-3-3 $\beta$  or 14-3-3 $\gamma$  in FALS patients.** A and B are the same sections as C and D, respectively. The identical LBHIs observed on H&E (A, B) in the anterior horn cells are intensely immunostained with 14-3-3 $\beta$  (C) and 14-3-3 $\gamma$  (D). Bar indicates 50  $\mu$ m.  
doi:10.1371/journal.pone.0020427.g002

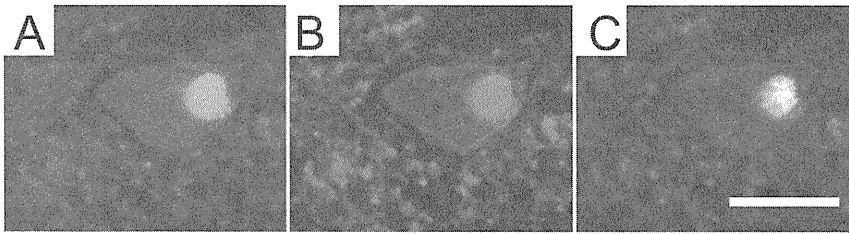


**Figure 3. A LBHI double-positive for 14-3-3 and SOD1 in a FALS patient.** A LBHI in an anterior horn cell is immunostained for pan 14-3-3 (A, green) and SOD1 (B, red), and the merged image is shown in C (yellow). Bar indicates 50  $\mu$ m.  
doi:10.1371/journal.pone.0020427.g003

#### Mutant SOD1 immunoreactivity in the mutant SOD1-Tg, the wild-type SOD1-Tg, and non-Tg wild-type mice

In mutant SOD1-Tg mice, C4F6 immunoreactivity was observed in the remaining anterior horn cells with cytoplasmic inclusions (Figure 4A). Immunoreactivity for C4F6 was restricted to the glial cells that were morphologically consistent with microglia in wild-type SOD1-Tg mice (Figure 4B) and absent in non-Tg wild-type mice (Figure 4C).

#### 14-3-3 immunoreactivity in the mutant SOD1-Tg, the wild-type SOD1-Tg, and non-Tg wild-type mice

Pan 14-3-3, 14-3-3 $\beta$  and 14-3-3 $\gamma$  immunoreactivities were grossly different between the mutant SOD1-Tg and the wild-type SOD1-Tg or non-Tg wild-type mice (Figure 5).

Such 14-3-3 immunoreactivities were strong in most of the remaining anterior horn cells of the mutant SOD1-Tg mice (Figure 5A, D, G), although they were not observed in the wild-type SOD1-Tg (Figure 5B, E, H) or non-Tg wild-type mice (Figure 5C, F, I).

#### Double immunofluorescent staining of C4F6 and 14-3-3 $\beta$ or 14-3-3 $\gamma$ in SOD1-Tg mice

As described above, the strong immunoreactivity of 14-3-3 $\beta$  and 14-3-3 $\gamma$  were observed in the mutant SOD1-Tg mice but not in the wild-type SOD1-Tg mice. Wherein, the distribution of immunoreactivity for C4F6, 14-3-3 $\beta$  and 14-3-3 $\gamma$  was analyzed.

All the three immunoreactivities were observed in the neuronal somata of the anterior horn cells. Furthermore, double immunofluorescent staining showed that both 14-3-3 $\beta$  and 14-3-3 $\gamma$  were partially co-localized with C4F6 in mutant SOD1-Tg mice (Figure 6).

In negative immunohistochemical controls, some sections were incubated with the primary antibody (0.2  $\mu$ g/ml) preabsorbed with an excess amount of the antigenic peptides, pan 14-3-3, 14-3-3 $\beta$  and 14-3-3 $\gamma$  (10  $\mu$ g/ml). No specific immunopositive staining was detected in these control sections.

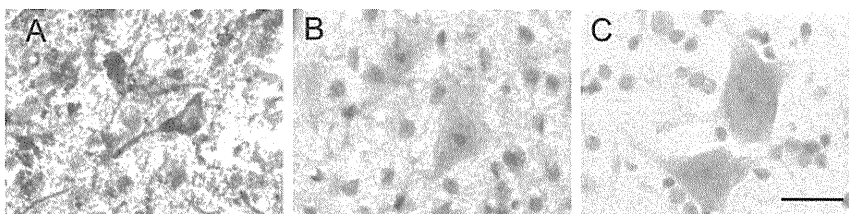


**Figure 4. Neuronal inclusions immunopositive for C4F6 in mice.** Strong immunoreactivity for C4F6 (A) was observed in the somatodendritic compartment with cytoplasmic inclusions in the mutant SOD1-Tg mice. Immunoreactivity for C4F6 was restricted to glial cells morphologically consistent with microglia in the wild-type SOD1-Tg mice (B) and absent in the non-Tg wild-type mice (C). Bar indicates 50  $\mu$ m.  
doi:10.1371/journal.pone.0020427.g004

#### Other 14-3-3 isoforms in the mutant SOD1-Tg mice and the wild-type SOD1-Tg mice

Immunoreactivity for 14-3-3 $\epsilon$ ,  $\eta$ ,  $\theta$ ,  $\sigma$ , and  $\zeta$  was observed in the neuronal somata and processes in the spinal cord. However, there were no remarkable differences in the distribution or intensity of the immunoreactivities between the mutant SOD1-Tg and wild-type SOD1-Tg mice.

#### Discussion

In this study, LBHIs in all FALS cases showed intense pan 14-3-3, 14-3-3 $\beta$  and 14-3-3 $\gamma$  immunoreactivities. Furthermore, the double immunofluorescent study showed 14-3-3 proteins were co-localized with SOD1 in LBHIs. Such distribution patterns were quite similar to those of the mutant SOD1-Tg mice. This is the first report that demonstrates a close relationship between 14-3-3 and SOD1 both in patients with FALS and mutant SOD1-Tg mice.

We have previously reported the localization of 14-3-3 proteins in the ubiquitinated intraneuronal inclusions in the anterior horn cells from patients with sporadic ALS [12]. We also already reported 14-3-3 immunoreactivity in the LBHIs in the anterior horn cells from a patient with FALS, with a two-base pair deletion in the SOD1 gene [19]; however, the co-localization of SOD1 and 14-3-3 was not assessed. Therefore the role of 14-3-3 proteins in LBHI formation with a SOD1 mutation has remained unclear. The co-localization of 14-3-3 and SOD1 in the LBHIs in both FALS patients and mutant SOD1-Tg mice suggested that 14-3-3 may play an important role in the formation of SOD1-containing LBHIs. The similar 14-3-3 positivity in the LBHI of sporadic ALS and FALS with SOD1 mutation further suggests that 14-3-3 is involved in the pathogenesis of ALS, irrespective of whether it is sporadic or familial.

Among the various isoforms of 14-3-3 protein, Kaneko and Hachiya proposed the possibility that a distinctive function of 14-3-3 $\zeta$  might be as a sweeper for misfolded proteins, such as aggregates or inclusion bodies [20]. Santpere et al. suggested that

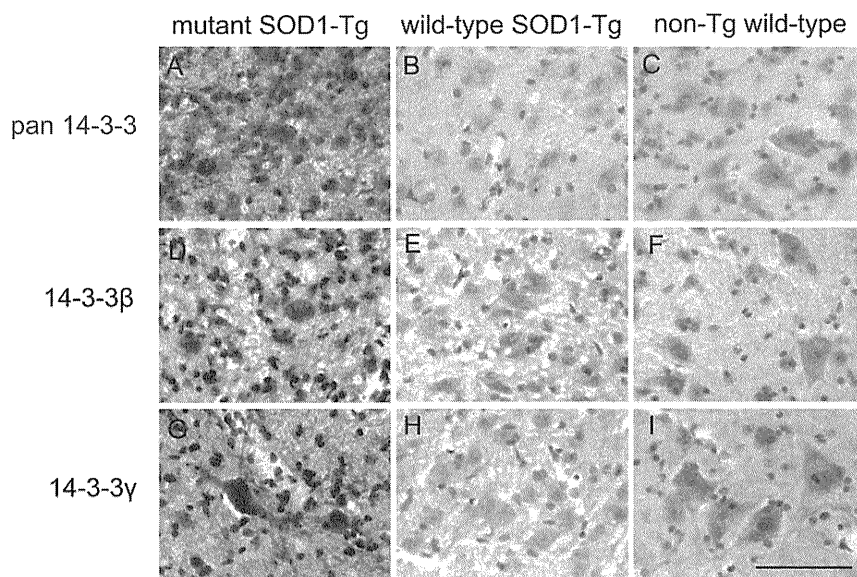


**Figure 5. Neuronal inclusions immunopositive for pan 14-3-3, 14-3-3 $\beta$ , and 14-3-3 $\gamma$  in the spinal cord of SOD1-Tg mice.** In mutant SOD1-Tg mice, strong immunoreactivity for pan 14-3-3 (A), 14-3-3 $\beta$  (D), and 14-3-3 $\gamma$  (G) were observed in the neuronal cytoplasm or neuronal process of the lumbar anterior horn cells. Such immunoreactivities were not observed in the wild-type SOD1-Tg (B, E, H) or non-Tg wild-type mice (C, F, I). Bar indicates 50  $\mu$ m.  
doi:10.1371/journal.pone.0020427.g005

the 14-3-3 $\gamma$  and 14-3-3 $\zeta$  isoforms may be the targets of oxidative damage in Alzheimer's disease [21], and some neurofibrillary tangles were reported to be immunolabeled with 14-3-3 $\beta$  and 14-3-3 $\gamma$  [22]. Similarly, 14-3-3 proteins have been co-localized in Lewy bodies [23] and in glial cytoplasmic inclusions from patients with multiple system atrophy [24]. In our recent study, 14-3-3 $\beta$  and 14-3-3 $\gamma$  were strongly expressed in the neuronal somata and processes of anterior horn cells in the spinal cord of mutant human  $\alpha$ -synuclein (A53T)-Tg mice, an animal model of Parkinson's

disease (PD) [25]. Therefore, 14-3-3 $\beta$  and 14-3-3 $\gamma$  may be the key isoforms associated with the formation of  $\alpha$ -synuclein- and SOD1-containing inclusions. This raises the possibility that there might be a common mechanism for inclusion formation at least between ALS and PD.

An insufficient function of the molecular chaperones may be directly involved in the loss of motor neurons in ALS [26,27]. Under non-pathological conditions, 14-3-3 proteins play important roles in signal transduction, apoptotic cell death and cell cycle

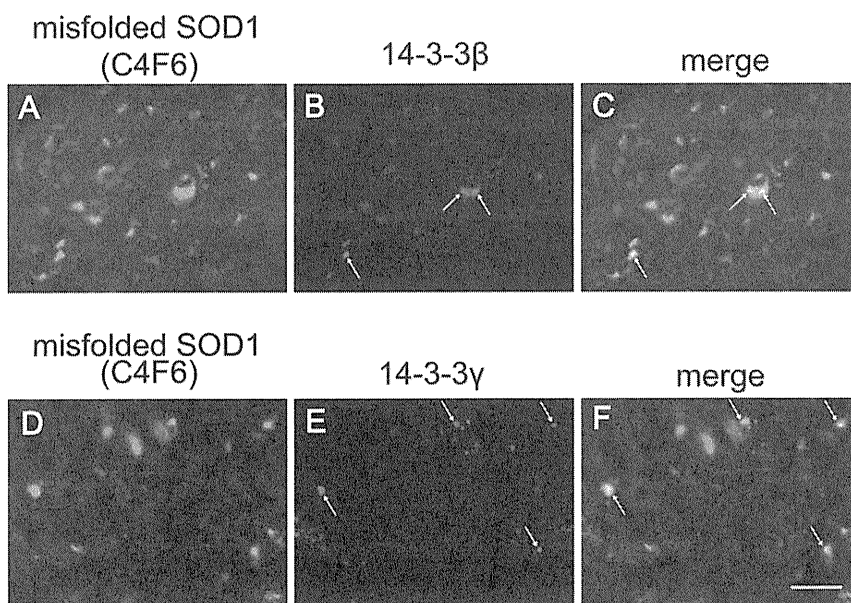


**Figure 6. Neuronal inclusions double-positive for C4F6 and 14-3-3 in the spinal cord of mutant SOD1-Tg mice.** Immunofluorescence for C4F6 (A, D, green), 14-3-3 $\beta$  (B, red), and 14-3-3 $\gamma$  (E, red), double immunofluorescence for C4F6 and 14-3-3 $\beta$  (C, merge), and double immunofluorescence for C4F6 and 14-3-3 $\gamma$  (F, merge) are shown in the anterior horn cells. Bar indicates 20  $\mu$ m.  
doi:10.1371/journal.pone.0020427.g006



control. 14-3-3 proteins inhibit apoptosis by binding to and inactivating pro-apoptotic proteins, including the mitochondrial Bcl-2 family member BAD, apoptosis signal-regulating kinase 1 (ASK1), and the Forkhead transcription factor FKHRL1 [10]. Therefore, the sequestration of 14-3-3 may cause neuronal dysfunction and thus contribute to cell death. Strong immunoreactivity for 14-3-3 in the LBHIs of FALS patients and in the mutant SOD1-Tg mice suggested that 14-3-3 proteins are trapped in the LBHIs, and this deficiency of the 14-3-3 proteins causes motor neuronal death in patient with FALS.

## References

- Byrne S, Walsh C, Lynch C, Bede P, Elamin M, et al. (2010) Rate of familial amyotrophic lateral sclerosis: a systematic review and meta-analysis. *J Neurol Neurosurg Psychiatry*.
- Rosen DR, Siddique T, Patterson D, Figlewicz DA, Sapp P, et al. (1993) Mutations in Cu/Zn superoxide dismutase gene are associated with familial amyotrophic lateral sclerosis. *Nature* 362: 59–62.
- Shibata N, Hirano A, Kobayashi M, Siddique T, Deng HX, et al. (1996) Intense superoxide dismutase-1 immunoreactivity in intracytoplasmic hyaline inclusions of familial amyotrophic lateral sclerosis with posterior column involvement. *J Neuropathol Exp Neurol* 55: 481–490.
- Rothstein JD (2009) Current hypotheses for the underlying biology of amyotrophic lateral sclerosis. *Ann Neurol* 65 Suppl 1: S3–9.
- Shibata N (2001) Transgenic mouse model for familial amyotrophic lateral sclerosis with superoxide dismutase-1 mutation. *Neuropathology* 21: 82–92.
- Murayama S, Ookawa Y, Mori H, Nakano I, Ihara Y, et al. (1989) Immunocytochemical and ultrastructural study of Lewy body-like hyaline inclusions in familial amyotrophic lateral sclerosis. *Acta Neuropathol* 78: 143–152.
- Mizusawa H, Matsumoto S, Yen SH, Hirano A, Rojas-Corona RR, et al. (1989) Focal accumulation of phosphorylated neurofilaments within anterior horn cell in familial amyotrophic lateral sclerosis. *Acta Neuropathol* 79: 37–43.
- Casareno RL, Waggoner D, Gitlin JD (1998) The copper chaperone CCS directly interacts with copper/zinc superoxide dismutase. *J Biol Chem* 273: 23625–23628.
- Boston PF, Jackson P, Thompson RJ (1982) Human 14-3-3 protein: radioimmunoassay, tissue distribution, and cerebrospinal fluid levels in patients with neurological disorders. *J Neurochem* 38: 1475–1482.
- Fu H, Subramanian RR, Masters SC (2000) 14-3-3 proteins: structure, function, and regulation. *Annu Rev Pharmacol Toxicol* 40: 617–647.
- Aitken A (1996) 14-3-3 and its possible role in co-ordinating multiple signalling pathways. *Trends Cell Biol* 6: 341–347.
- Kawamoto Y, Akiguchi I, Nakamura S, Budka H (2004) 14-3-3 proteins in Lewy body-like hyaline inclusions in patients with sporadic amyotrophic lateral sclerosis. *Acta Neuropathol* 108: 531–537.
- Malaspina A, Kaushik N, de Belleruche J (2000) A 14-3-3 mRNA is up-regulated in amyotrophic lateral sclerosis spinal cord. *J Neurochem* 75: 2511–2520.
- Nakano I, Hirano A, Kurland LT (1984) Familial amyotrophic lateral sclerosis: Neuropathology of two brothers in American “C” family. *Neurol Med(Tokyo)* 20: 458–471.
- Hirano A, Kurland LT, Sayre GP (1967) Familial amyotrophic lateral sclerosis. A subgroup characterized by posterior and spinocerebellar tract involvement and hyaline inclusions in the anterior horn cells. *Arch Neurol* 16: 232–243.
- Gurney ME, Pu H, Chiu AY, Dal Canto MC, Polchow CY, et al. (1994) Motor neuron degeneration in mice that express a human Cu,Zn superoxide dismutase mutation. *Science* 264: 1772–1775.
- Ceballos-Picot I, Nicole A, Briand P, Grimber G, Delacourte A, et al. (1991) Neuronal-specific expression of human copper-zinc superoxide dismutase gene in transgenic mice: animal model of gene dosage effects in Down’s syndrome. *Brain Res* 552: 198–214.
- Urushitani M, Ezzi SA, Julien JP (2007) Therapeutic effects of immunization with mutant superoxide dismutase in mice models of amyotrophic lateral sclerosis. *Proc Natl Acad Sci U S A* 104: 2495–2500.
- Kawamoto Y, Akiguchi I, Fujimura H, Shirakashi Y, Honjo Y, et al. (2005) 14-3-3 proteins in Lewy body-like hyaline inclusions in a patient with familial amyotrophic lateral sclerosis with a two-base pair deletion in the Cu/Zn superoxide dismutase (SOD1) gene. *Acta Neuropathol* 110: 203–204.
- Kaneko K, Hachiya NS (2006) The alternative role of 14-3-3 zeta as a sweeper of misfolded proteins in disease conditions. *Med Hypotheses* 67: 169–171.
- Santpere G, Ferrer I (2009) Retracted: “Oxidative damage of 14-3-3 zeta and gamma isoforms in Alzheimer’s disease and cerebral amyloid angiopathy” [*Neuroscience* 146 (2007) 1640–1651]. *Neuroscience* 161: 663.
- Umahara T, Uchihara T, Tsuchiya K, Nakamura A, Iwamoto T, et al. (2004) 14-3-3 proteins and zeta isoform containing neurofibrillary tangles in patients with Alzheimer’s disease. *Acta Neuropathol* 108: 279–286.
- Berg D, Riess O, Bornemann A (2003) Specification of 14-3-3 proteins in Lewy bodies. *Ann Neurol* 54: 135.
- Kawamoto Y, Akiguchi I, Nakamura S, Budka H (2002) Accumulation of 14-3-3 proteins in glial cytoplasmic inclusions in multiple system atrophy. *Ann Neurol* 52: 722–731.
- Shirakashi Y, Kawamoto Y, Tomimoto H, Takahashi R, Ihara M (2006) alpha-Synuclein is colocalized with 14-3-3 and synphilin-1 in A53T transgenic mice. *Acta Neuropathol* 112: 681–689.
- Bruening W, Roy J, Giasson B, Figlewicz DA, Mushynski WE, et al. (1999) Up-regulation of protein chaperones preserves viability of cells expressing toxic Cu/Zn-superoxide dismutase mutants associated with amyotrophic lateral sclerosis. *J Neurochem* 72: 693–699.
- Yamashita H, Kawamata J, Okawa K, Kanki R, Nakamizo T, et al. (2007) Heat-shock protein 105 interacts with and suppresses aggregation of mutant Cu/Zn superoxide dismutase: clues to a possible strategy for treating ALS. *J Neurochem* 102: 1497–1505.

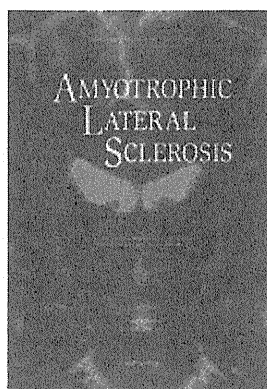
## Acknowledgments

We would like to express our cordial gratitude to Ms. Hitomi Nakabayashi for her excellent technical assistance, and Dr. Ahmad Khundakar for his critical reading of the manuscript.

## Author Contributions

Conceived and designed the experiments: MI HT HI SS RT. Performed the experiments: YO YS YK UM MO. Analyzed the data: YO MI. Contributed reagents/materials/analysis tools: SK HY AH. Wrote the paper: YO MI.

## Amyotrophic Lateral Sclerosis



### Protein Disulfide Isomerase immunopositive Inclusions in patients with Amyotrophic lateral Sclerosis

Journal:	<i>Amyotrophic Lateral Sclerosis</i>
Manuscript ID:	MALS-2011-0045.R2
Manuscript Type:	Original Article
Date Submitted by the Author:	30-May-2011
Complete List of Authors:	Honjo, Yasuyuki; Kyoto university, Pharmacoepidemiology; Kyoto university, Neurology Kaneko, Satoshi; Kansai medical university, Neurology Ito, Hidefumi; Kyoto university, Neurology Horibe, Tomohisa; Kyoto university, Pharmacoepidemiology Nagashima, Masato; Kansai medical university, Neurology Nakamura, Masataka; Kansai medical university, Neurology Fujita, Kengo; Kansai medical university, Neurology Takahashi, Ryosuke; Kyoto university, Neurology Kusaka, Hirofumi; Kansai medical university, Neurology Kawakami, Koji; Kyoto university, Pharmacoepidemiology
Keywords:	Amyotrophic lateral sclerosis, protein disulfide isomerase, Lewy body like hyaline inclusion, misfolded protein, unfolded protein response

SCHOLARONE™  
Manuscripts

URL: <http://mc.manuscriptcentral.com/als> Email: [gerd.halvorsen@informa.com](mailto:gerd.halvorsen@informa.com)

1  
2  
3  
4  
5  
6  
7  
8  
9  
10  
11  
12  
13  
14  
15  
16  
17  
18  
19  
20  
21  
22  
23  
24  
25  
26  
27  
28  
29  
30  
31  
32  
33  
34  
35  
36  
37  
38  
39  
40  
41  
42  
43  
44  
45  
46  
47  
48  
49  
50  
51  
52  
53  
54  
55  
56  
57  
58  
59  
60

# Protein Disulfide Isomerase immunopositive Inclusions in patients with Amyotrophic lateral Sclerosis

Yasuyuki Honjo<sup>1,2</sup>, Satoshi Kaneko<sup>3</sup>, Hidefumi Ito<sup>2</sup>, Tomohisa Horibe<sup>1</sup>,  
Masato Nagashima<sup>3</sup>, Masataka Nakamura<sup>3</sup>, Kengo Fujita<sup>3</sup>, Ryosuke  
Takahashi<sup>2</sup>, Hirofumi Kusaka<sup>3</sup>, Koji Kawakami<sup>1</sup>

<sup>1</sup> *Department of Pharmacoepidemiology, Graduate School of Medicine and Public Health, Kyoto University.*

<sup>2</sup> *Department of Neurology, Faculty of Medicine, Kyoto University.*

<sup>3</sup> *Department of Neurology, Kansai Medical University.*

**Correspondence:** Koji Kawakami, MD, PhD (Corresponding author). Professor and Chairman.

Department of Pharmacoepidemiology School of Medicine and Public Health Kyoto University

Yoshida Konoecho, Sakyo-ku, Kyoto 606-8501, Japan Phone: +81-75-753-4459, Fax:

+81-75-753-4469 E-mail: [kawakami.koji.4e@kyoto-u.ac.jp](mailto:kawakami.koji.4e@kyoto-u.ac.jp)

**Key words:** *Amyotrophic lateral sclerosis, protein disulfide isomerase, Lewy body-like hyaline inclusion, misfolded protein, unfolded protein response*

**Running title:** PDI-immunopositive inclusions in patients with ALS

## Abstract

**Objective:** The major pathological hallmarks of amyotrophic lateral sclerosis (ALS) are neuronal cytoplasmic inclusions (NCIs) and swollen neurites. Superoxide dismutase (SOD) 1-immunopositive NCIs are observed in patients with familial ALS (FALS) and TAR DNA-binding protein 43kDa (TDP-43)-immunopositive NCIs are found in patients with sporadic ALS (SALS). Protein disulfide isomerase (PDI) is a member of the thioredoxin superfamily and is believed to accelerate the folding of disulfide-bonded proteins by catalyzing the disulfide interchange reaction, which is the rate-limiting step during protein folding in the luminal space of the endoplasmic reticulum. **Methods:** Post-mortem spinal cord specimens from five patients with SALS and one with FALS (I113T), and five normal controls were utilized in this immunohistochemical study. **Results:** We found PDI-immunopositive swollen neurites and NCIs in the patients with ALS. Furthermore, PDI was co-localized with TDP-43 and SOD1 in NCIs. The accumulation of misfolding proteins may disturb axon transport and make swollen neurites. As the motor neuron is the longest cell in the nervous system, the motor system may selectively be disturbed. **Conclusions:** We assume that PDI is S-nitrosylated in the affected neurons, which inhibits its enzymatic activity and thus allows protein misfolding to occur in ALS.

## Introduction

Amyotrophic lateral sclerosis (ALS) is a major neurodegenerative disease but there is currently no effective treatment available because the etiology or mechanism of ALS is still unclear. In general, 90-95% patients with the disease are sporadic ALS (SALS) and 5-10% are familial ALS (FALS) patients (1). In a gene analysis study, approximately 20% of FALS patients had a mutation in Cu/Zn-superoxide dismutase (SOD) 1 (1). But SOD1 deficiency does not make ALS, because SOD1-knockout mice do not reveal any obvious phenotype (2). In contrast, transgenic mice expressing human SOD1 containing a mutation develop a motor neuron disease similar to FALS (3). These results suggested that the accumulation of SOD1 is toxic for neurons and is linked to the pathogenesis of ALS. In fact, SOD1 transgenic mice are commonly used as a model for ALS.

The major pathological changes of ALS are neuronal cytoplasmic inclusions (NCIs) and swollen axons, which are called spheroid. Lewy body-like hyaline inclusions (LBHIs) in SALS and conglomerate inclusions in FALS are specific NCIs in ALS and both are a major pathological hallmark of ALS. TAR DNA-binding protein 43kDa (TDP-43) is the major component of LBHIs and is seen in patients with ALS (1). Recently, a human TDP-43 transgenic mouse has been reported (4). The transgenic

1  
2  
3  
4  
5  
6  
7 mice, expressing high levels of human TDP-43, displayed severe neurological  
8  
9  
10 alterations and died prematurely at 5 months of age. In addition, the mice developed  
11  
12  
13 progressive accumulation of inclusions in neurons, but the inclusions were not  
14  
15  
16 immunopositive for TDP-43, implying the involvement of other unknown factors than  
17  
18  
19 TDP-43. TDP-43 is not only the protein to contributing to the pathology of SALS.  
20  
21  
22

23 Protein disulfide isomerase (PDI) is a member of the thioredoxin superfamily  
24  
25  
26 and is believed to accelerate the folding of disulfide-bonded proteins by catalyzing the  
27  
28  
29 disulfide interchange reaction, which is the rate-limiting step during protein folding in  
30  
31  
32 the luminal space of the endoplasmic reticulum (ER) (5,6). Such exchange reactions can  
33  
34  
35 occur intramolecularly, leading to rearrangement of disulfide bonds in a single protein.  
36  
37  
38 The second major function of PDI is as a chaperone to unfold cholera toxin (7). This  
39  
40  
41 is independent of its first function in disulfide exchange. NO-induced S-nitrosylation of  
42  
43  
44 PDI inhibits its enzymatic activity, leading to the accumulation of polyubiquitinated  
45  
46  
47 proteins in patients with SALS and ALS model mice (8). Furthermore, overexpression  
48  
49  
50 of PDI decreased mutant SOD1 aggregation, inclusion formation, ER stress induction,  
51  
52  
53 and toxicity, whereas small interfering RNA targeting PDI increased mutant SOD1  
54  
55  
56 inclusion formation, indicating a protective role for PDI against SOD1 misfolding (8).  
57  
58  
59  
60

1  
2  
3  
4  
5  
6  
7 In this study, we identified anti-PDI-antibody immunopositive NCIs in the  
8  
9 spinal cord of patients with ALS. Furthermore, we found PDI-immunopositive swollen  
10  
11 neurites in the spinal cord of patients with ALS. In addition, TDP-43 and SOD1 were  
12  
13 co-localized with PDI in NCIs of patients with ALS. The accumulation of misfolded  
14  
15 proteins such as SOD1 and TDP-43 is toxic for motor neurons and PDI may be involved  
16  
17  
18  
19  
20  
21  
22 in NCIs.  
23  
24  
25  
26  
27  
28  
29

## 30 **Material and Methods**

### 31 *Tissue preparation*

32  
33  
34  
35  
36  
37  
38 Postmortem spinal cord specimens from five patients with SALS and one with FALS  
39  
40 (I113T), and five normal control were utilized in this study. All patients gave informed  
41  
42 consent and this study was approved by the local ethics committee. The diagnosis of the  
43  
44 patients was defined by pathological study. Specimens from the spinal cord and  
45  
46  
47  
48 brainstem were obtained from the autopsied spinal cord of the normal control and ALS  
49  
50  
51 patients. All samples were fixed in 10% neutral formalin at room temperature. Several  
52  
53  
54  
55  
56  
57  
58  
59  
60 paraffin-embedded tissue blocks were prepared and cut into 7  $\mu$ m-thick sections on a  
microtome. The paraffin-embedded sections were deparaffinized in xylene, followed by

1  
2  
3  
4  
5  
6 rehydration in ethanol solutions of decreasing concentration as previously described  
7  
8  
9 (9,10).  
10  
11  
12  
13

### 14 15 16 *Immunohistochemistry* 17

18 Immunohistochemical staining was performed as previously described (9,10).  
19  
20

21  
22 Immunohistochemical staining for PDI was performed using polyclonal rabbit anti-PDI  
23  
24 antibody that has been described before (11-13). Monoclonal mouse anti-TDP-43  
25  
26 antibody was purchased from Abnova (Taipei, Taiwan) and mouse anti-human SOD1  
27  
28 antibody was purchased from R&D systems, Inc. (Minneapolis, MN, USA). The  
29  
30 sections were incubated in a microwave oven for a few minutes after which the sections  
31  
32 were incubated in 0.3% hydrogen peroxide in 0.1 M PBS at room temperature for 30  
33  
34 min to block the endogenous peroxidase activity. After washing with PBS containing  
35  
36 0.3% Triton X100 (PBST) the sections were incubated overnight with the primary  
37  
38 antibody diluted in PBST at room temperature. A dilution of 1:100 was used for the  
39  
40 primary PDI antibody. After incubation with the primary antibody and washing, the  
41  
42 sections were incubated with the secondary antibody (diluted 1:100). The sections were  
43  
44 incubated with an avidin biotin complex, and were allowed to react with a solution  
45  
46 containing 0.02% 3,3'-diaminobenzidine tetrahydrochloride (DAB), 0.005% hydrogen  
47  
48  
49  
50  
51  
52  
53  
54  
55  
56  
57  
58  
59  
60



1  
2  
3  
4  
5  
6  
7 peroxide, and 0.6% nickel acetate in 0.05 M Tris/HCl buffer.  
8  
9

10  
11  
12  
13 *Double staining of PDI and human TDP-43 in tissue sections from SALS samples*  
14

15  
16 To confirm the anatomical relationship between PDI and human TDP-43, we performed  
17  
18 a double-staining study using mouse anti-TDP-43 antibody and rabbit anti-PDI antibody  
19  
20 as described in (9). Briefly, sections of the spinal cords were incubated in medium  
21  
22 containing anti-TDP-43 and anti-PDI antibodies (each diluted 1:100) in PBST overnight  
23  
24 at room temperature. After washing, the sections were reacted with the secondary  
25  
26 antibodies consisting of polyclonal goat anti-rabbit immunoglobulins/FITC (The  
27  
28 Jackson Laboratory, Bar Harbor, ME, USA) and polyclonal swine anti-mouse  
29  
30 immunoglobulins/TRITC (Cosmo Bio Science, San Diego, CA, USA) for 1 h at room  
31  
32 temperature. After rinsing, the slides were mounted Vectashield (Vector Laboratories,  
33  
34 Burlingame, CA, USA) and photographed using an Olympus Fr1000D: FV/IX81  
35  
36 (Olympus corporation, Tokyo, Japan) confocal laser scanning microscope. We selected  
37  
38 15 TDP-43-immunopositive NCIs in the immunostained sections of the spinal cord  
39  
40 from each of three patients with SALS. We then counted the number of  
41  
42 PDI-immunopositive NCIs in the selected TDP-43-immunopositive NCIs from each  
43  
44 patient.  
45  
46  
47  
48  
49  
50  
51  
52  
53  
54  
55  
56  
57  
58  
59  
60

1  
2  
3  
4  
5  
6  
7  
8  
9  
10 *Double staining of PDI and SOD1 in FALS samples*

11  
12 Double staining using anti-PDI antibody and anti-SOD1 antibody was performed as  
13 described above. We selected 15 SOD1-immunopositive NCIs in the immunostained  
14  
15  
16  
17  
18  
19 sections of the spinal cord from the patient with FALS. We then counted the number of  
20  
21  
22 PDI-immunopositive NCIs in the selected SOD1-immunopositive NCIs from the  
23  
24  
25 patient.  
26  
27  
28  
29  
30

31 **Results**

32  
33  
34 *PDI-immunopositive neuronal cells*

35  
36  
37 In the control specimens, many neurons were immunopositive for the anti-PDI antibody.  
38  
39  
40 PDI immunoreactivity was typically observed in the neuronal bodies and dendrites, but  
41  
42  
43 nuclei were not stained (Figure 1, panels A,B). In addition, some of the  
44  
45  
46 oligodendrocytes were also immunopositive using anti-PDI antibody (Figure 1, panel B).  
47  
48  
49 Some of astrocytes were PDI-immunopositive, but they were stained weakly. In the  
50  
51  
52 tissue sections from patients with SALS and FALS, we detected numerous  
53  
54  
55 PDI-immunopositive NCIs (Figure 2, panels A,B). These PDI-immunopositive NCIs  
56  
57  
58 were observed in all patients with SALS and FALS. Furthermore, we found  
59  
60

1  
2  
3  
4  
5  
6  
7 anti-PDI-antibody-immunopositive swollen neurites in SALS and FALS samples  
8  
9  
10 (Figure 3, panels A,B). Other immunoreactivity of anti-PDI antibody was not markedly  
11  
12  
13 different between the normal and ALS patients.  
14  
15  
16  
17

#### 18 *Double staining of PDI and TDP-43 in SALS samples*

19  
20  
21  
22 Immunohistochemical double staining for PDI and TDP-43 showed that PDI and  
23  
24  
25 TDP-43 were co-localized in the NCIs of SALS samples (Figure 4). The number of  
26  
27  
28 NCIs labeled by antibodies to PDI was smaller than the number of  
29  
30  
31 TDP-43-immunopositive NCIs (Figure 4). A quantitative examination revealed that  
32  
33  
34 approximately 93% of the TDP-43-immunopositive NCIs were also  
35  
36  
37 PDI-immunoreactive. The proportion of PDI-immunopositive NCIs compared with  
38  
39  
40 TDP-43-immunopositive NCIs was not remarkably different among patients.  
41  
42  
43  
44  
45  
46

#### 47 *Double staining of PDI and SOD1 in FALS samples*

48  
49  
50 Immunohistochemical double staining for PDI and SOD1 showed that PDI and SOD1  
51  
52  
53 were co-localized in the NCIs of FALS samples (Figure 5). The number of NCIs labeled  
54  
55  
56 by antibodies to PDI was less than the number of SOD1-immunopositive NCIs. A  
57  
58  
59 quantitative examination revealed that approximately 73% of the  
60

1  
2  
3  
4  
5  
6 SOD1-immunopositive NCIs were also PDI-immunoreactive.  
7  
8  
9

## 10 11 12 Discussion

13  
14  
15 The accumulation of misfolded, aggregated proteins and  $\text{Ca}^{2+}$  influx can cause  
16 ER stress in neurons (5). ER stress signaling, otherwise known as the unfolded protein  
17 response (UPR), is triggered by an increased load of misfolded proteins in the organelle.  
18  
19 In SOD1 (L84V) transgenic mice, the aggregation of ER and numerous free ribosomes  
20 was observed associated with abnormal inclusion-like structures in spinal cord neurons  
21 at the presymptomatic stage (14). Furthermore, the induction of LBHIs *in vitro* by ER  
22 stress in neuroblastoma cells was revealed and the inclusions were closely similar to  
23 LBHIs in patients with SOD1-linked FALS (14). The accumulation of SOD1 can cause  
24 ER stress and that may cause apoptosis of neuronal cells in FALS.  
25  
26  
27  
28  
29  
30  
31  
32  
33  
34  
35  
36  
37  
38  
39  
40  
41  
42

43  
44 Mutant SOD1 specifically interacted with Derlin-1, a component of  
45 ER-associated degradation (ERAD) machinery and triggered ER stress through  
46 dysfunction of ERAD (15). Mutant SOD1-induced ER stress activated apoptosis.  
47  
48 Perturbation of binding between mutant SOD1 and Derlin-1 by Derlin-1-derived  
49 oligopeptide suppressed mutant SOD1-induced ER stress and motor neuron death (15).  
50  
51  
52  
53  
54  
55  
56  
57  
58  
59 In addition, Derlin-1 overexpression reduced mutant SOD1-induced cell toxicity and  
60